Bulletin de la Société Royale des Sciences de Liège, Vol. 80, 2011, p. 229 - 234

Physical Properties and Evolutionary Stages of Massive Young Stellar Objects in the Large Magellanic Cloud

C.-H. Rosie Chen[1], Remy Indebetouw[1,2], Jonathan P. Seale[3], Leslie W. Looney[3], You-Hua Chu[3], Robert A. Gruendl[3] and Barbara A. Whitney[4]

[1] University of Virginia, Charlottesville, Virginia, U.S.A.
[2] National Radio Astronomical Observatory, Charlottesville, Virginia, U.S.A.
[3] University of Illinois, Urbana, Illinois, U.S.A.
[4] Space Science Institute, Boulder, Colorado, U.S.A.

Abstract: Massive stars drive the evolution of galactic interstellar media, yet their formation remains poorly understood. We use *Spitzer* Infrared Spectrometer (IRS) observations of 277 massive young stellar objects (YSOs) in the Large Magellanic Cloud (LMC) and combine them with multi-wavelength photometry from U to 70 μm to construct and model their spectral energy distribution (SED) and to deduce their mass and evolutionary stage. We also examine the immediate interstellar and stellar environment using high-resolution optical and near-IR images to assess the origin of dust emission and multiplicity of sources. Some of these YSOs are spatially coincident with known masers and ultracompact H II regions that can be used as an independent check on the feasibility of SED fits. Comparisons among YSOs' physical properties, immediate stellar and interstellar environment, and mid-IR spectral features are used to discuss evolution of massive YSOs in the LMC.

1 Introduction

Despite the fact that massive stars are one of the main energy sources of the interstellar medium (ISM) and hence play a key role in the evolution of their host galaxies, the processes of their formation remain not well understood. It has been challenging to observationally study these processes due to large distances, high extinction, and short timescales of critical evolutionary phases (e.g., Zinnecker & Yorke 2007). It is also difficult to model theoretically as the collapse timescale is so short that a massive star begins to produce high radiation pressure when it is still accreting, making accretion onto a star with mass $\geq 40 M_{\odot}$ difficult. Thus an alternate scenario such as mergers of lower-mass ones (Bonnell et al. 1997) or pressure release via outflow cavities (Krumholz et al. 2009) may be required.

High sensitivity *Spitzer* mid-IR observations make it possible for large surveys of massive YSOs to provide observational constraints such as relative timescales of evolutionary phases. This requires a well-defined classification system that can reflect the evolution of massive YSOs. The LMC, due to its proximity (50 kpc) and nearly face-on orientation, is an excellent laboratory as YSOs are at known, common distances and can be resolved. Its low metallicity (1/3 $Z_{\odot}$) also provides a chance to

investigate how that affects star formation. A large sample of massive YSOs has been detected in the LMC (Whitney et al. 2008; Gruendl & Chu 2009). Classifying these YSOs needs extra care as they can be multiples or small clusters unresolved by *Spitzer*'s 2″-resolution, i.e., 0.5 pc in the LMC. As demonstrated in our previous studies, the common method of comparing observed SEDs to predictions from single YSO models is a good approximation for YSOs that appear single or are dominant sources within the *Spitzer* resolution, but not for otherwise cases (Chen et al. 2009, 2010). We have then developed an empirical scheme using combined diagnoses of SEDs and immediate interstellar environment. Meanwhile, mid-IR spectral features are used to classify YSOs with *Spitzer* IRS observations (Seale et al. 2009). Each of these three schemes has its own perspectives in classifying YSOs. We thus use our large IRS sample to carry out a systematic study to examine how these classifications compare to one another and how they are linked to the evolutionary sequence of YSOs.

2 Data Reduction and Analysis

We use *Spitzer* IRS observations of 277 massive YSOs in the LMC, by far the largest mid-IR spectroscopic sample of confirmed extragalactic YSOs (Seale et al. 2009), to study their physical properties and evolutionary stages. To construct SEDs of these YSOs, we have used the IR catalog from Gruendl & Chu (2009), expanded it to include MCPS and IRSF catalogs in the optical and near-IR wavelengths (Zaritsky et al. 2004; Kato et al. 2007), and combined these photometric data with corresponding IRS spectra (Seale et al. 2009). To incorporate IRS spectra in the SED fitter (Robitaille et al. 2007), we extracted 11 data points at carefully selected wavelengths to delineate silicate feature and the underlying continuum (Chen et al. 2011, in prep.). Fig. 1 demonstrated that the model fits are better constrained with the SED composed of both photometric data and IRS spectrum than that of only photometric data. The inferred physical properties such as masses and evolutionary stages thus have smaller uncertainties for a critical examination. Each YSO is classified with three schemes summarized below.

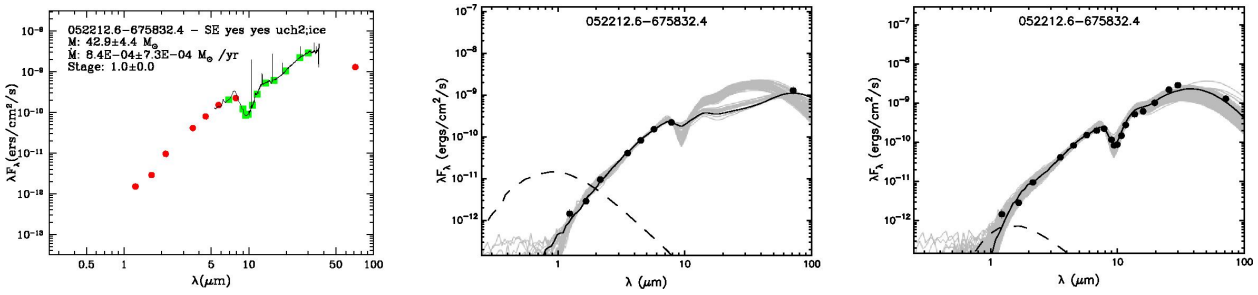

Figure 1: Left: An example of a YSO's SED with combined data of broadband photometry (red dots) and IRS spectra (solid lines). Data points extracted from the IRS spectrum for model fits are marked in green dots. Middle: Model fits (solid and gray lines) to the example YSO whose SED is composed of only photometric data (black dots). Right: Models fits (solid and gray lines) to the same YSO whose SED is composed of data points from both photometry and IRS data points (black dots). It is evident that the fits are better constrained with data points around the 10-μm silicate absorption.

Stage I/II/III – quantitative scheme using predictions from radiative transfer codes with dust distribution analogous to Class I/II/III (Robitaille et al. 2006). Classification is based on inferred envelope accretion rate ($\dot{M}_{\rm env}$) and disk mass ($M_{\rm disk}$) normalized to stellar mass ($M_\star$). Stage I YSOs have significant infalling envelopes and possibly disks and thus $\dot{M}_{\rm env}/M_\star > 10^{-6}$/yr. Stage II YSOs have optically thick disks and possibly remnant envelopes and thus $\dot{M}_{\rm env}/M_\star < 10^{-6}$/yr and $M_{\rm disk}/M_\star > 10^{-6}$. Stage III have optically thin disks and thus $\dot{M}_{\rm env}/M_\star < 10^{-6}$/yr and

$M_{\rm disk}/M_\star < 10^{-6}$. The scheme is physical but the applicability depends on geometry of dust distribution and relation between the observable envelope mass and $\dot{M}_{\rm env}$.

Type I/II/III – empirical scheme using SEDs and interstellar environments (Chen et al. 2009). Type I YSOs have SED with a steep rise from the near-IR to 24 μm as the radiation is mostly from their circumstellar envelopes; they are generally not visible at optical or J band, but visible in the K band and bright at 24–70 μm. Type II YSOs have SEDs with a low peak in the optical and a high peak at 8–24 μm corresponding to the stellar core and the circumstellar disk, respectively, after the envelope has dissipated; they are faint in the optical, but bright in the J band to 8 μm, and then faint again at the 24 μm. Type III YSOs have SEDs peaking in the optical with modest amounts of dust emission in the near- to mid-IR as they are largely exposed but still possess remnant circumstellar material; their brightness fades in the longer wavelength and they are often surrounded by H II regions.

Type S/SE/P/PE/E/F – empirical scheme using mid-IR spectral features: S – 10 μm silicate absorption, P – 5-10 and 10-13 μm polycyclic aromatic hydrocarbon (PAH) emission, and E – 10-20 μm ion fine-structure lines (Seale et al. 2009). YSOs are classified by their major spectral features into six groups: S, SE, P, PE, E, and F. S and SE groups have strong silicate absorption, indicating that they are highly embedded sources and most likely at earliest evolutionary stage. P, PE, and E groups have spectra dominated by UV-emitting central objects and are thus likely at later evolutionary stages. For YSOs in this sample, we adopted the classification results from Seale et al. (2009).

3 Toward a Consistent Evolutionary Picture of Massive YSOs

3.1 Physical Properties of YSOs vs. Formation of Ultracompact H II Regions

Massive stars inject energy into the surroundings even during their formation. They can ionize the circumstellar gas to form small, dense H II regions such as ultracompact H II regions (UCHIIs). Among the 277 YSOs in the sample, 20 are spatially coincident with UCHIIs identified by compact radio continuum sources (Indebetouw et al. 2004). The link between YSOs and UCHIIs allows us to compare the YSOs' evolutionary stages inferred from SED models to the circumstellar conditions required to form UCHIIs, providing an independent check for the feasibility of SED models.

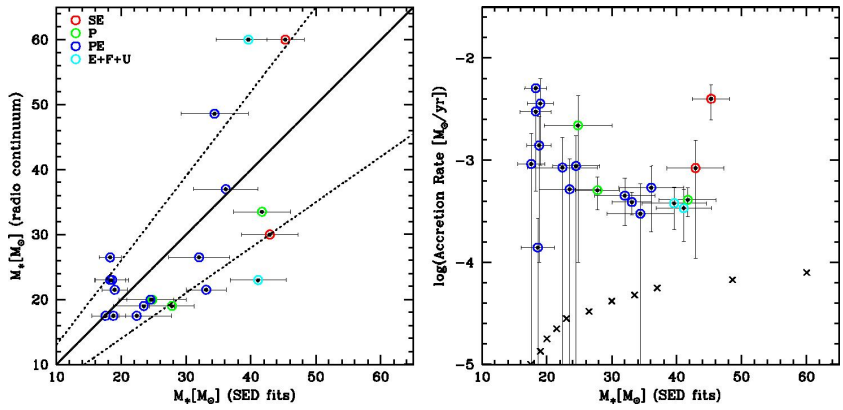

Figure 2: Left: Comparisons between masses inferred from SED fits and radio continuum (Indebetouw et al. 2004) for 20 YSOs that are counterparts of UCHIIs. Error bars from SED fits are marked. IRS spectral types of these YSOs are marked with additional circles in different colors (see legends). Masses estimated from these two methods are generally in good agreement within 30%, as indicated with dotted lines. Right: $\dot{M}_{\rm env}$ vs. $M_\star$ of YSOs inferred from SED fits (circles and error bars) compared to $\dot{M}_{\rm crit}$ of stars expected for certain masses (crosses; Churchwell 2002).

Masses of these 20 sources can be determined independently for YSOs and UCHIIs, providing a consistency check. For YSOs, masses are inferred from model fits to their SEDs. For UCHIIs, assuming the relationship for main-sequence stars, masses can be translated from spectral types implied by the ionizing fluxes determined from radio continuum emission. Fig. 2 shows that except a few outliers, agreement exists between masses estimated using these two methods within 30%. The discrepancies in outliers with masses $\geq 50 M_{\odot}$ from radio continuum are artificial since the upper mass limit in pre-calculated YSO models is 50 $M_{\odot}$. The discrepancies in the opposite cases likely indicate a non-negligible leakage of ionizing fluxes in UCHIIs.

The development of a UCHII depends not only on the ionizing flux provided by the central star, but also on the opacity of the circumstellar material. For infalling rates higher than some critical values, $\dot{M}_{\rm crit}$, the circumstellar medium will have such opacity that the ionized region will be too small and optically too thick to be detectable (Churchwell 2002). Fig. 2 shows that 70% (14 of 20) of the YSOs have inferred $\dot{M}_{\rm env} \gg \dot{M}_{\rm crit}$, similar to what was found in a smaller sample from our previous studies (Chen et al. 2009, 2010). Two possible causes have been suggested. One is that most of the infalling envelope material is used in forming an accretion disk as modeled by Yorke & Sonnhalter (2002), and the ionization radiation escapes in the polar directions. The other is that at the LMC distance, it is difficult to distinguish bound, circumstellar dust from the more distant but still heated interstellar dust. Several UCHIIs are Type III YSOs that have formed small H II regions visible in Hα images. Thus, their high $\dot{M}_{\rm env}$ mostly suggests that they still have abundant dust/gas in the surroundings. Lastly, compared to YSOs' IR spectral types, UCHIIs are found in all but the most embedded S-type, suggesting that they can form at very early stage and possibly accrete via hypercompact H II regions (Keto & Wood 2006). Confirmation would need higher resolution cm data and near-IR spectra.

3.2 Evolutionary Stages of Massive YSOs

The results of SED fits to YSOs are shown in Fig. 3. These YSOs are massive with $M_{\star}$ = 8–45$M_{\odot}$, and $\sim 90\%$ of them are Stage I sources with $\dot{M}_{\rm env}/M_{\star} \sim 10^{-6}$–$10^{-3}$/yr. These high $\dot{M}_{\rm env}/M_{\star}$ qualifies them as Stage I. However, as $> 50\%$ of them show optical counterparts or small H II regions, i.e., Types II or III YSOs using our empirical scheme, the inferred $\dot{M}_{\rm env}/M_{\star}$ appears more indicative of abundant dust than true accretion rates. Nonetheless, some of the Type I YSOs with high $\dot{M}_{\rm env}/M_{\star}$ are likely to be actively accreting. The highest $\dot{M}_{\rm env}/M_{\star} \sim 10^{-3}$/yr are found in YSOs with 10–20$M_{\odot}$ but not higher masses, suggesting that some of them might be younger counterparts in the process of accreting onto more massive ones. However the true accretion rates are yet to be estimated from independent methods such as outflow strengths. On the other hand, as aforementioned that $\sim 60\%$ of the YSOs are multiples, $\dot{M}_{\rm env}/M_{\star}$ for such sources are more relevant to accretion onto a compact (size < 0.5 pc) cluster. The high $\dot{M}_{\rm env}/M_{\star}$ is consistent with the accretion rate $\sim 10^{-3} M_{\odot}$/yr in models of cluster formation (Tan & McKee 2002). This small cluster mode of forming massive stars appears to be prevalent in both the Galaxy and the LMC, despite their metallicity difference.

Comparisons of IR spectral types to other classifications show that YSOs of S/SE-type or with ice absorption feature all have $\dot{M}_{\rm env}/M_{\star} \geq 10^{-5} M_{\odot}$/yr, qualitatively consistent with what is expected for massive, dense envelopes from which these spectral features arise. YSOs of P/PE-type have $\dot{M}_{\rm env}/M_{\star} \sim 10^{-6} - 10^{-3}$/yr, however, as more than half of them are Types II and III YSOs, the high $\dot{M}_{\rm env}/M_{\star}$ in some cases may have been raised due to inclusion of dust emission from H II regions. Examining IR spectral types of known masers and UCHIIs shows that only small fractions, i.e., 13% (=1/8) in masers and 15% (=3/20) in UCHIIs respectively, are embedded YSOs of SE-type or with ice absorption, while most of them are more evolved YSOs of P/PE-types. Masers and UCHIIs in the LMC appear to preferentially develop at later evolutionary stages.

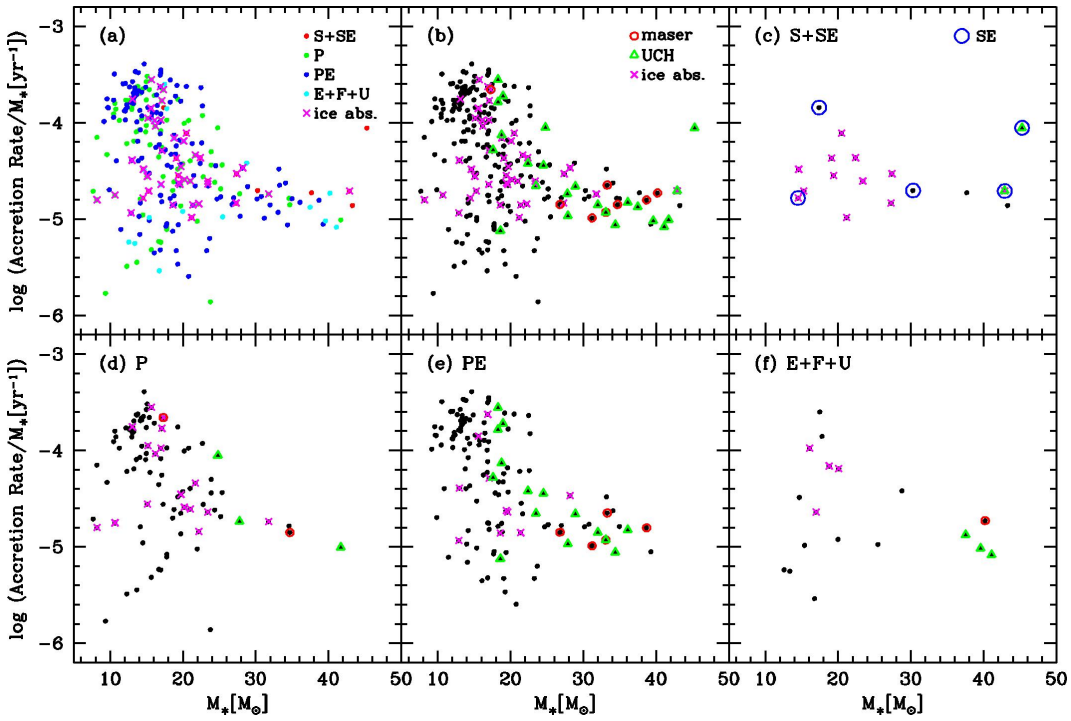

Figure 3: $\dot{M}_{\rm env}$ vs. $M_\star$ inferred from model fits to 277 YSOs with IRS spectra. (a) YSOs of different spectral classifications (Seale et al. 2009) are marked in different colors as shown in legends. YSO with ice absorption features are marked with additional crosses. (b) YSOs (black dots) that are counterparts of masers and UCHII (Green et al. 2008; Indebetouw et al. 2004) are marked with additional circles and triangles, respectively. (c-f) YSOs of different IR spectral types shown in separate panels for clarity. Symbols are the same as in (b) except extra blue circles for SE-type in (c).

Acknowledgements

This work is supported through NASA grants JPL 1282653 and 1288328.

References

Bonnell, I. A., Bate, M. R., Clarke, C. J. & Pringle, J. E. 1997, MNRAS, 285, 201
Chen, C.-H. R., Chu, Y.-H., Gruendl, R. A., Gordon, K. D. & Heitsch, F. 2009, ApJ, 695, 511
Chen, C.-H. R., Indebetouw, R., Chu, Y.-H., Gruendl, R. A., Testor, G., Heitsch, F., Seale, J. P, Meixner, M., et al. 2010, ApJ, 721, 1206
Churchwell, E. 2002, ARAA, 40, 27
Green, J. A., Caswell, J. L., Fuller, G. A., Breen, S. L., Brooks, K. Burton, M. G., Chrysostomou, A. Cox, J., et al. 2008, MNRAS, 385, 948
Gruendl, R. A., & Chu, Y. 2009, ApJS, 184, 172
Indebetouw, R., Johnson, K. E., & Conti, P. 2004, AJ, 128, 2206
Kato, D., Nagashima, C.; Nagayama, T., Kurita, M., Koerwer, J. F., Kawai, T., Yamamuro, T., Zenno, T., et al. 2007, PASJ, 59, 615
Keto, E., & Wood, K. 2006, ApJ, 637, 850
Krumholz, M. R., Klein, R. I., McKee, C. F., Offner, S. S. R. & Cunningham, A. J. 2009, Science, 323, 754
Robitaille, T. P., Whitney, B. A., Indebetouw, R., & Wood, K. 2007, ApJS, 169, 328
Robitaille, T. P., Whitney, B. A., Indebetouw, R., Wood, K. & Denzmore, P. 2006, ApJS, 167, 256
Seale, J. P., Looney, L. W., Chu, Y.-H., Gruendl, R. A., Brandl, B., Chen, C.-H. R., Brandner, W. & Blake, G. A. 2009, ApJ, 699, 150
Tan, J. C. & McKee, C. F. 2002, Hot Star Workshop III: The Earliest Phases of Massive Star Birth, 267, 267

Whitney, B. A., Sewilo, M., Indebetouw, R., Robitaille, T. P., Meixner, M., Gordon, K., Meade, M. R., Babler, B. L., et al. 2008, AJ, 136, 18
Yorke, H. W., & Sonnhalter, C. 2002, ApJ, 569, 846
Zaritsky, D., Harris, J., Thompson, I. B. & Grebel, E. K. 2004, AJ, 128, 1606
Zinnecker, H. & Yorke, H. W. 2007, ARAA, 45, 481

Discussion

H. Beuther: How can you be sure that some are single objects? At the given spatial resolution of $\sim$ 0.25 parsec, all objects should consist of at least small clusters...
R. Chen: We have examined the highest resolution of near-IR images, i.e. CTIO 4m or VLT NACO, available for these YSOs; those "single" sources appear as single point sources in these images. While we think it is possible that these "single" sources may have undetected low-mass young stars around them, or unresolved massive binary companion, the luminosities of these sources are dominated by one (or two in binary case) YSOs. The "multiple" sources have no obvious dominant YSOs and are considered as groups or clusters of massive YSOs. We focus on the contrast between these types of YSOs.

C. Martayan: At lower metallicity, it should be easier to form more massive stars. Do you have a mass-distribution for the YSOs in the LMC and MW? Are they different? I would expect some differences between the distributions with the metallicity.
R. Chen: I have made mass functions of massive YSOs in two H II regions in the LMC, N 44 & N 159, and found that in N 44 the slope of the mass function is consistent with the Salpeter value, while in N 159, the slope is more shallow. This shallow slope is likely to be biased by the higher detection limit of lower mass YSOs due to the bright background. We are working on getting physical properties of larger samples of YSOs in H II regions to examine whether there the IMF is shallower in the LMC.